In presenting this dissertation as a partial fulfillment of the requirements for an advanced degree from the Georgia Institute of Technology, I agree that the Library of the Institution shall make it available for inspection and circulation in accordance with the regulations governing materials of this type. I agree that permission to copy from, or to publish from, this dissertation may be granted by the professor under whose direction it was written, or, in his absence, by the Dean of the Graduate Division when such copying or publication is solely for scholarly purposes and does not involve potential financial gain. It is understood that copying from, or publication of, this dissertation which involves potential financial gain will not be allowed without written permission.

Lewis A. Safar

EFFECT OF HEATING UPON MASS FLOW RATE THROUGH PORTS OF A MANIFOLD

A THESIS

Presented to

the Faculty of the Graduate Division

by

Lewis Anthony Safar

In Partial Fulfillment

of the Requirements for the Degree

Master of Science in Mechanical Engineering

Georgia Institute of Technology

January 1957

EFFECT OF HEATING UPON MASS FLOW RATE THROUGH

PORTS OF A MANIFOLD

Approved: [signature]

[signature]

Date Approved by Chairman: 23 January 1957

ACKNOWLEDGMENTS

I wish to express my sincere gratitude to Dr. Thomas W. Jackson for his assistance, suggestions, and encouragement as my thesis adviser. I am also indebted to the other members of my committee, Dr. Henderson C. Ward and Professor Kenneth G. Picha, for their helpful suggestions and criticism of the paper. I would like to thank Mrs. Wanda Reaves for preparing the final manuscript and tables. I would also like to thank Mr. Thomas D. Sangster for his assistance in assembling the apparatus.

TABLE OF CONTENTS

LIST OF TABLES

LIST OF ILLUSTRATIONS

SUMMARY

The investigation was conducted primarily to determine the effect of heating upon the mass rate of flow through a port of a manifold. Coincident with the primary investigation, the change of static pressure along the manifold length was also studied.

An appropriate apparatus was designed and constructed to determine the effect of heating upon the mass flow rate of air through a port. The port to be heated was wrapped with electrical resistance heaters, and power was supplied through two Powerstat transformers. Several tests were performed with the heated port located in various openings of the manifold. These tests were compared to the tests made when none of the ports were heated.

Whenever heat was supplied to a port through which air was flowing, the volume rate of flow increased due to the density of the fluid decreasing. On the other hand, however, the mass rate of flow of the air decreased through a port when heat was supplied to that port. This occurrence can be attributed to the fact that the density of the fluid decreased at a faster rate than the rate at which the velocity of the fluid increased. Also, since the viscosity of the air increased with rising temperatures, the shearing stresses within the fluid increased tending to retard the flow.

The trends of the static pressure along the manifold length and the volume rates of flow when none of the ports were heated are discussed. Both the static pressures and the volume flow rates increased in the

direction of flow in all cases. Two important factors which determine the flow distribution in manifolds are (a) the friction of the fluid against the internal surface of the main channel, and (b) the momentum of the main fluid stream. In the tests conducted the pressure rise due to the momentum of the main fluid stream was greater than the pressure drop due to friction of the air against the internal surface of the main channel.

The flow of air throughout the main channel and ports was turbulent and the flow was fully developed before entering the first port.

CHAPTER I

INTRODUCTION

A manifold is a pipe with a number of inlets or outlets through which fluid is flowing. The practicality of the manifold has been demonstrated numerous times. Examples are the familiar pipe burner for gaseous fuels; headers or manifolds for certain types of multitube air heaters; the manifold of a gasoline engine; and distributing pipes in water-filtering systems.

Although many mathematical difficulties have been encountered, some progress has been made in solving manifold problems. The problem of flow through a pipe with a porous wall has been studied by Olson (1).* He derived the differential equations for the pressure drop and flow and indicated the relationship between the two quantities. Dow (2) carried out a theoretical analysis for the flow through a perforated pipe with a closed end for the special case of a constant linear rate of discharge along the length of the pipe. The validity of the theoretical results was verified by experiment. Keller (3) studied the general problems of a manifold discharging fluid through several openings distributed along the manifold length, and supplying fluids to a set of parallel pipes or ducts. A study of the variation of static pressure along the main channel of a manifold has been carried out by Acrivos, Babcock, and Pigford (4). Analyses were made of a "blowing" manifold in which the fluid flowing through the main channel undergoes a subdivision, and of a "sucking"

---

*Numbers in parentheses identify references listed in bibliography.

manifold in which the fluid enters the main channel from the various openings.

The purpose of this investigation was to determine the effect of heating upon mass flow through ports of a manifold. This involved the analysis of experimental data obtained from an apparatus designed to supply air to seven ports in a manifold with one of the ports being heated.

CHAPTER II

PRELIMINARY INVESTIGATIONS

The case of variation of discharge with uniformly spaced holes has been examined by Keller (5). A typical example of this is the ordinary pipe burner, shown schematically in Figure 1*.

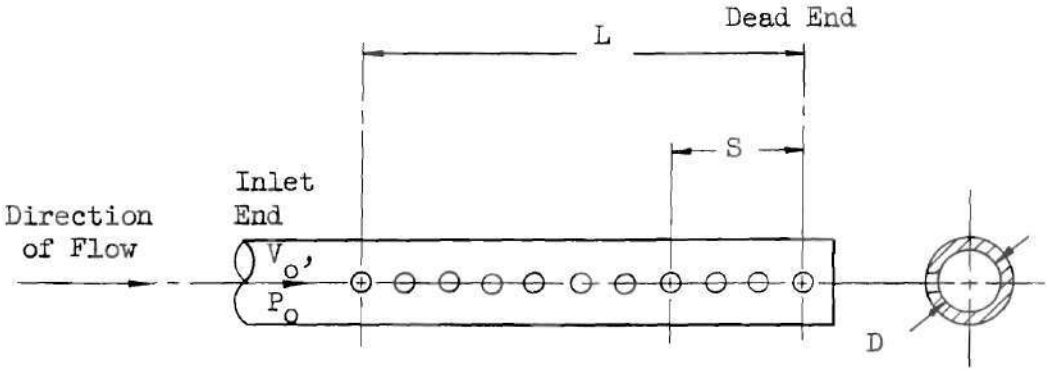

Figure 1. Typical Pipe Burner

Keller has pointed out that there are two dimensionless ratios which define such a manifold, namely, the ratio of active length to diameter or L/D, and the area ratio, or

$$\frac{\text{Sum of areas of all discharge openings}}{\text{Cross-sectional area of manifold}}$$

The fundamental equation relating pressure and flow to position along the manifold reduces to the following second-order differential equation for which no solution has yet been found:

---

*For clarity all other figures have been placed in Appendix B.

$$\left(\frac{A}{Kw}\right)^2 \left(\frac{d^2V}{ds^2}\right) = -V + \left(\frac{f}{D}\right)\left[\frac{V^2}{(dV/ds)}\right]$$

where

A = cross-sectional area of manifold, sq. ft.

K = coefficient of discharge at openings in manifold

w = width of discharge slot in manifold, ft.

V = longitudinal velocity in manifold, ft. per sec.

s = distance from dead end of manifold, ft.

f = coefficient of friction

D = diameter, ft.

Keller assumed a reasonably large number of holes and calculated the values section by section, starting with unit velocity and pressure at the discharge hole nearest the dead end of the manifold and working back from hole to hole toward the inlet end. The results of his numerical work are shown in Figure 2.

The manufacturers of pipe burners have stated that the area ratio should not exceed unity but this takes no account of the effect of variation of the L/D ratio. Keller proceeds to show the variation of discharge in Figure 2 when various L/D and area ratios are used.

Keller also made an analysis of the variation of flow through manifolded ducts. He assumed the ducts to be of equal diameter and length, and evenly spaced along the manifold. The flow distribution he found is similar to that for the case shown in Figure 2, with the exception of a reduction of the equivalent area ratio due to the resistance of the ducts. Taking the discharge coefficient for the holes as 0.62, and that at

entrance to the ducts as 0.75, with a friction coefficient of 0.00052g, he showed that for ducts of the same diameter as the holes

$$\text{Area ratio for ducts} =$$

$$(\text{area ratio for holes}) \times \frac{1}{\sqrt{0.6834 + 0.0129(L_t/D_t)}}$$

where

L_t = length of a duct

D_t = diameter of a duct

If the fluid is a gas which is heated or cooled in passing through the tubes or ducts, a further correction must be made for the increased or decreased resistance resulting from the change of velocity and density. Keller did not consider this case.

Acrivos, Babcock, and Pigford (6) have also studied the problem of flow distributions in manifolds. Their numerical solutions of applicable equations resulted in predictions of flow variation. Several tests were performed in order to compare the predicted flow non-uniformity with experimentally observed distributions. The predicted and observed flow distributions were in approximate agreement.

CHAPTER III

APPARATUS

The inlet air system.--Air for the tests was supplied by a single stage Type "F" American Blower Company pressure fan, Model 6-28. The fan was powered by a fifteen horsepower, 3500 RPM motor, and provided 640 cubic feet of free air per minute at a pressure of 53 inches of water. The volume of air flowing was controlled by a conical valve in the ten inch inlet duct of the fan.

From the outlet of the fan the air passed into a section of six-inch steel pipe 80 inches long. This was connected to a 24-inch length of the same diameter pipe by pressure tap flanges (see Figures 3 and 4). An orifice plate for measuring the flow of air in the pipe was placed between the two flanges. In order to keep the length of pipe between the fan and the orifice to a minimum a straightening vane was installed in the 80-inch length of pipe in accordance with the recommendations of Stearns, Jackson, Johnson, and Larson (7). The vane was constructed from nineteen 12-inch lengths of one-inch diameter thin wall tubing. The tubes were soldered into a bundle and held in the six-inch pipe by two set screws. The outlet of the vane was located 37 inches upstream from the orifice plate. Twenty-four inches downstream of the orifice the air passed into a three-inch diameter pipe 83 inches long.

Test section.--One end of the three-inch pipe test section was threaded and a flange was welded to the other end. The flanged end was bolted to a flange on the six-inch pipe. An end cap was placed on the threaded end

of the three-inch pipe. Seven one-inch diameter pipe couplings were brazed in a line on the three-inch pipe. The distance between center lines of the pipe couplings was four inches. The center line of the last pipe coupling was four inches from the closed end of the three-inch pipe. A 1.0625-inch hole was drilled through the three-inch pipe at the center of each pipe coupling. Seven one-inch diameter steel pipes were each cut to a length of 15 inches. One end of each pipe was threaded and each one was screwed into a pipe coupling (see Figure 5).

Seven one-eighth-inch diameter holes were drilled in the manifold for measuring static pressures. These holes were drilled in planes perpendicular to the manifold and passing through the center lines of the pipe couplings. The holes were located 90 degrees from the pipe couplings. One-quarter-inch nipples, each approximately one inch long, were brazed around the holes. A rubber tube was connected to the first nipple and to a three-way connection. Another rubber tube was connected to the three-way connection and to an eight inch Prandtl micromanometer. A third rubber tube joined the three-way connection to a "U" tube water manometer (see Figures 3 and 6). Due to this connection the static pressure at section one could be found.

Both ends of a one-inch diameter steel pipe approximately 20 inches long were threaded and a cap placed on each end. A nipple was inserted in one cap and a rubber tube was connected from the nipple to the reservoir of the micromanometer. Six holes, one-eighth-inch diameter, were drilled in the one-inch pipe and a nipple was brazed around each hole. Six rubber tubes connected the six nipples of the three-inch pipe to the six nipples of the one-inch pipe. A bleed valve was also inserted on the one-inch pipe. With any five rubber tubes clamped, a pressure differential between

section one and any other section could be determined. Therefore, the static pressure at any other section could be found by adding the pressure differential to the gage pressure of section one.

Flow meters.--One orifice flowmeter and one pitot tube were incorporated in the apparatus. The orifice meter was placed in the six-inch diameter pipe to measure the amount of air entering the test section. The orifice meter was a flange tap installation with one-half-inch pressure taps located one inch upstream and one inch downstream from the center of the orifice plate. The flanges, gaskets and orifice plate were made by the Foxboro Company, Foxboro, Massachusetts, and installed in accordance with the manufacturers instructions.* The pressure differential across the orifice plate and the static pressure upstream from the plate were measured by "U" tube water manometers.

A 7/32-inch diameter pitot tube was used to determine the stagnation pressure at the exit of each port. A rubber tube was connected from the pitot tube to an eight-inch Prandtl micromanometer. Since the pressure range was expected to be greater than eight inches of water, an extension was constructed and installed as shown in Figure 7. The distance between the hairlines of the two sight glasses was found experimentally to be 7.839 inches.

Thermocouples.--Four number 28 gage chromel-alumel thermocouples were used to measure the wall temperature of the port to be heated. The locations of the thermocouple junctions are shown in Figure 5. Four very small holes were drilled in the wall of the pipe and the junctions were inserted

*The Foxboro Company, Foxboro, Massachusetts, bulletin 6-110 dated July 1941.

in each hole. The metal around the holes was peened with a center punch in order to secure the thermocouple junctions. The leads of the four thermocouples were extended along the pipe wall and brought out from the top of the pipe to be connected to a junction block.

A fifth thermocouple was used to measure the temperature of the air entering the ports. This thermocouple was located 11 inches upstream from port number one with the junction in the center of the main channel.

The thermocouple EMF's were measured by a Portable Precision Potentiometer, number 8662, manufactured by Leeds and Northrup and using an ice bath cold junction.

Heat source.--Two lengths of 20-gage nichrome wire were coiled on the port to be heated. A layer of asbestos tape insulated the 34-foot inside coil from the pipe. Another layer of asbestos tape insulated the inside coil from the 37-foot outside coil. A transite block was installed on each end of the port. The leads from the coiled wires were clamped to bolts on both blocks. A layer of fiber glass insulated the heaters from the atmosphere.

The electrical power system for the heaters consisted of two Powerstat Variable Transformers, type S649, manufactured by Superior Electric Company. A diagram of the electrical heater circuits is shown in Figure 8.

Miscellaneous equipment.--A barometer, a 220°F mercury thermometer, and a 400°F mercury thermometer were also used during the investigation.

CHAPTER IV

TEST PROCEDURE

To begin a run the motor powering the pressure fan was started and the quantity of air entering the manifold was governed by the position of the conical valve. The desired flow rate could be obtained quickly knowing the pressure differential across the orifice and temperature and static pressure before the orifice.

There were five tests made with each test consisting of five runs. The total mass flow rate was varied in each of the runs. An attempt was made to keep the total flow rate constant for the corresponding run of each test. One run was selected from random to be reproduced in order to determine the accuracy of the equipment.

None of the ports were heated during the first test. When the system reached equilibrium, readings were made of the temperature and static pressure before the orifice, pressure differential across the orifice, inlet and outlet temperatures of the ports, static pressures along the manifold length, stagnation pressure at the exit of each port, and barometric pressure.

Port number one was heated during the second test. After the total flow rate had been set for a run, power was gradually applied to the heaters by varying the voltage through the Powerstat transformers. Since a voltmeter was connected in parallel to each heater and an ammeter in series in each circuit, an indication of the heat supplied could be determined. The maximum amount of power was applied in order to get the

highest possible temperature rise through the port. Additional data taken during this test were the temperature of the air out of the heated port and the wall temperatures of the heated port.

Errors in the reading of the air outlet temperatures of the heated ports were due to radiation from the pipe wall and the location of the thermometer in the air stream. These readings were accurate within approximately six degrees Fahrenheit. It was estimated that the readings of the wall temperatures of the heated ports were accurate within five degrees Fahrenheit.

Tests three, four, and five consisted of heating ports three, five, and seven, respectively. The same data taken in test two were taken in these three tests.

Since the maximum range of the micromanometer used for finding the static pressure along the manifold length was only eight inches of water, the pressure at each port could not be found directly. It was therefore necessary to find the static pressure at port one by means of a "U" tube manometer. With this reading as a reference, the pressure differential between the other ports and port one was determined with the micromanometer. Each pressure differential was added to the value found at port one so that the static pressure along the manifold could be determined. The pressure differential readings were accurate within approximately 0.004 inches of water.

An eight-inch Prandtl micromanometer was also used to find the stagnation pressure. Previous to the tests, it was known that the stagnation pressure range would be higher than eight inches of water. Hence, an extension was brazed to the sight glass holder of the micromanometer with another sight glass at the top of the extension. Whenever

a reading was less than eight inches of water, the water level was taken at the hairline of the bottom sight glass. When the reading was above eight inches of water, the water level was taken at the hairline of the top sight glass. This reading was added to the distance between the two hairlines to obtain the correct stagnation pressure. The accuracy of the stagnation pressure readings was approximately $\pm$ 0.004 inches of water.

CHAPTER V

ANALYSIS OF EXPERIMENTAL RESULTS

General.--Two important factors which determine the flow distribution in and from manifolds are (a) the friction of the fluid against the internal surface of the main channel, and (b) the momentum of the main fluid stream. The latter corresponds to change in velocity head. In general, as the fluid flows along the manifold, its axial velocity decreases due to part of the fluid being discharged laterally through the openings. Therefore the fluid in the manifold is being decelerated and, in accordance with Bernoulli's theorem, this tends to increase the fluid pressure. On the other hand, friction causes a pressure drop along the manifold length. The relative magnitudes of the pressure gain due to deceleration and the pressure loss due to friction determine whether the pressure rises or falls from the inlet end to the closed end of the manifold.

The change in pressure in the direction of flow in a manifold is given by the equation

$$dp = \left[- \frac{d(v^2)}{2\beta v} \right] + \left[\frac{f}{\beta} \left(\frac{ds}{D} \right) \left(\frac{v^2}{v} \right) \right]$$

when s is measured from the closed end. The sign of the first or deceleration term is negative because increase of pressure corresponds to decrease of velocity; the sign of the second or friction term is positive because, although friction always causes a decrease of pressure in the direction of flow, ds also is negative in the direction of flow.

Assumptions.--In carrying out the experimental work, several assumptions had to be made. Since it was desired to find the trend of the static pressure along the manifold, pressure taps were inserted at cross-sections in line with the center line of each port, and at right angles to each port. It is obvious that the pressure is not constant along each cross-section. It was therefore assumed that the pressures found were the averages for each cross-section.

In order to simplify the experimental work, only one outlet temperature of the non-heated ports was taken for each run. It was assumed that this temperature represented the outlet temperatures of all of the non-heated ports. For the instrumentation used, a variation in temperature could not be detected, so that this assumption was a valid one.

After the maximum velocity out of each port was found, it was necessary to know the average velocity in order to find the flow rate out of each port. Since the total flow rate was known, a constant, a, was found such that this constant times the maximum velocity gave the average velocity. It was assumed that this constant held for the range of Reynolds numbers for all ports of a given run.

Discussion of results.--The governing equation for determining the maximum velocity at the exit of the ports of the manifold is

$$P_t = P_s + \frac{\rho U^2}{2\beta}$$

or

$$U = \sqrt{\frac{2\beta(P_t - P_s)}{\rho}}$$

It can be seen from the experimental data that the stagnation pressure increased whenever a port was heated. However, it can be seen in Figures 9, 10, 11, 12, and 13 that the mass rate of flow decreased through the heated ports. The mass flow rate was determined by the equation

$$W_p = \rho A \bar{u}$$

Since the mass flow rate through a port decreases with heating, it is evident that the density of the fluid decreased at a faster rate than the rate at which the velocity of the fluid increased. Another factor which influenced the mass rate of flow is the viscosity. Since the dynamic viscosity μ and the kinematic viscosity ν increase with rising temperature for gases, the shearing stresses within the fluid increased tending to retard the flow. In the system investigated the effects due to viscosity changes were small.

For the range of Reynolds numbers obtained in the tests, Schlichting (8) gives a value of ~0.81 for the constant, a, the average velocity divided by the port maximum or center line velocity. However, the pitot tube probe when placed at several points on the cross-section of a port outlet indicated that the velocity profile was slightly skewed. This made it necessary to calculate a particular constant, a, for each run of each test. The method of determining the constant, a, is shown in Appendix D. The constant varied from 0.847 to 0.874 for the tests.

The trends of static pressure along the manifold length and the volume flow rates for the tests though similar to those obtained by Acrivos, Babcock, and Pigford, are not identically comparable because the systems are not geometrically similar. The results of run number

three with none of the ports heated were selected as an example of this investigation. Comparisons between the example selected and the values obtained by Acrivos, Babcock, and Pigford are shown in Figures 14 and 15.

The results of this investigation are in agreement with the numerical results obtained by Keller in determining the distribution of discharge along the manifold length. Taking the first run with none of the ports heated as a representative sample of this investigation, the results of the run are shown as curve 6 of Figure 2. In this investigation, the area ratio was 0.84 and the L/D ratio was 7.82.

CHAPTER VI

CONCLUSIONS AND RECOMMENDATIONS

Conclusions.--The most important conclusion that can be drawn from this investigation is that the mass rate of flow through a port of the manifold decreased when heat was transferred to the fluid flowing through that port. This occurrence was due to the fact that the density of the fluid decreased at a faster rate than the rate at which the velocity of the fluid increased.

The trends of the static pressure along the manifold length and the volume rates of flow for the tests were compared to those obtained experimentally by Acrivos, Babcock, and Pigford. In general the static pressure in the direction of flow increased in all cases because the pressure rise due to the momentum of the main fluid stream overcame the pressure drop due to friction of the fluid against the internal surface of the main channel.

Recommendations.--The total mass rates of flow for air in the tests ranged from approximately 0.288 lb./sec. to 0.544 lb./sec. It is suggested that this investigation be extended to total flow rates above and below these figures.

In continuing the experiments with air, it is recommended that the apparatus be redesigned. Changes to be considered are a smaller diameter for the main channel and ports of smaller diameter. Since the velocity profile of the fluid leaving the ports was slightly skewed, it is recommended that the length-to-diameter ratio of the ports be at least

20 to 1. This would also make it possible to obtain a higher temperature rise of the fluid flowing through the ports.

Additional work with ports at various angles to the main channel is also desirable.

APPENDIX A

LIST OF SYMBOLS

LIST OF SYMBOLS

a	Constant $\bar{u}/U$
A	Cross-sectional area
C	Coefficient of discharge, inlet air orifice
D	Diameter
D_1	Inlet air pipe diameter
D_2	Inlet air orifice diameter
E_1, E_2, E_3, E_4	Millivolt readings of thermocouples along heated port, numerals denoting thermocouple locations
E_{ip}	Millivolt reading of thermocouple at inlet to ports
f	Coefficient of friction
g	Gravity acceleration, 32.2 ft./sec.^{2}
h_1	Orifice pressure differential
h_{s_1}, h_{s_2}, h_{s_3}, h_{s_4}, h_{s_5}, h_{s_6}, and h_{s_7}	Static pressures along manifold length at test section, numerals denoting port number
h_{s_o}	Upstream static pressure, inlet air orifice
K	Coefficient of discharge at openings in manifold
K_1	Orifice flow coefficient
L	Length
P_b	Barometric pressure
P_s	Static pressure
P_t	Stagnation pressure
R	Gas constant for air
s	Distance from dead end of manifold
T_c	Temperature out of non-heated ports

T_h	Temperature out of heated port
T_{ip}	Temperature inlet to ports
T_o	Upstream temperature, inlet air orifice
T_1, T_2, T_3, T_4	Wall temperatures of heated ports, numerals denoting thermocouple locations
$\bar{u}$	Average velocity at exit of port
U	Center line velocity
v	Specific volume
V	Longitudinal velocity in manifold
w	Width of discharge slot in manifold
W_p	Mass flow rate at exit of port
W_t	Mass of air flow, inlet air orifice
β	Dimensional constant 32.2 $lb_m ft/lb_f sec^2$
γ	$D_2/D_1 = 0.5$
μ	Dynamic viscosity
ν	Kinematic viscosity
ρ	Density
ρ_1	Upstream air density, inlet air orifice
$\sum$	Summation

APPENDIX B

FIGURES

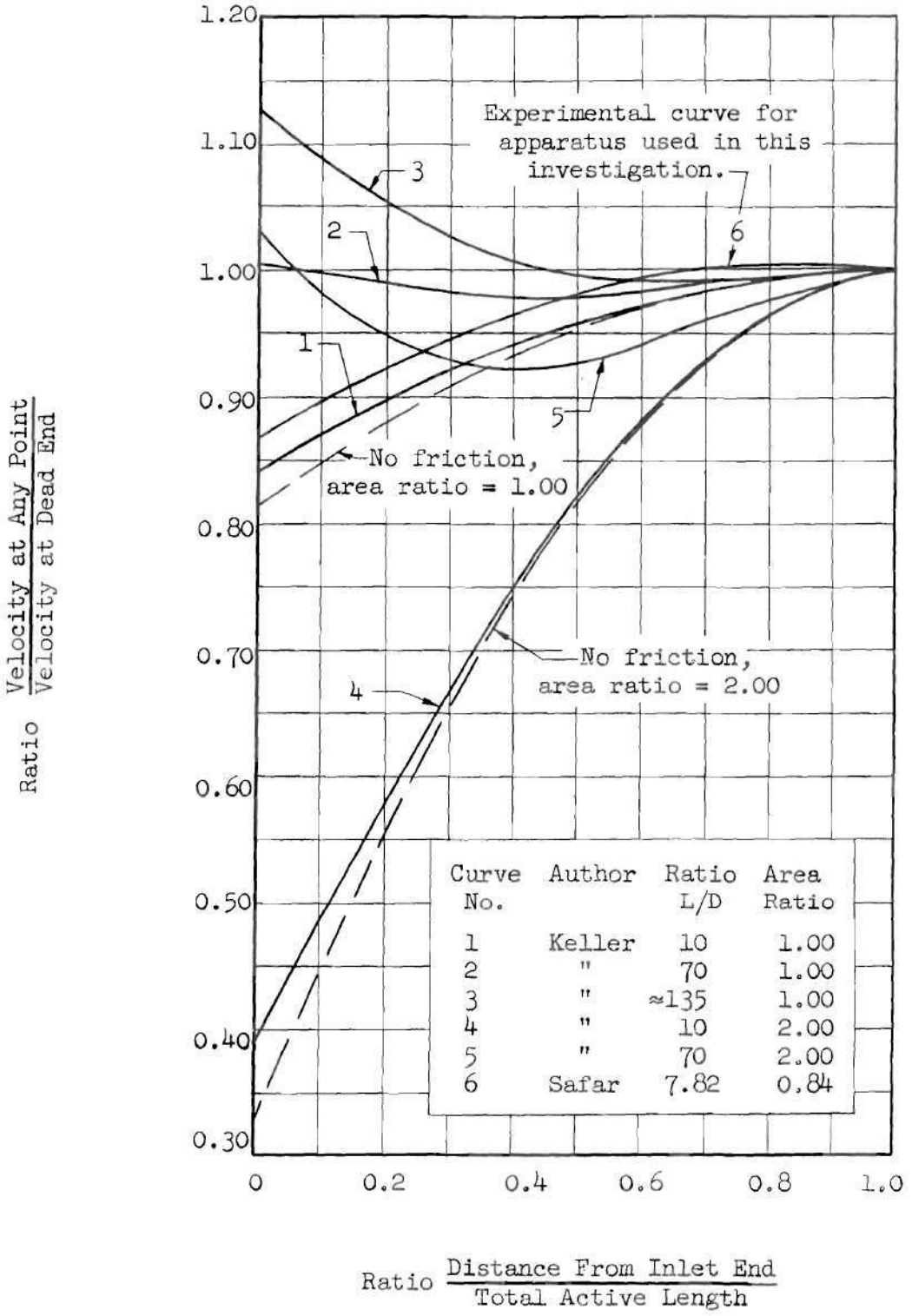

Figure 2. Distribution of Discharge Along Length of Manifold of Constant Cross Section; f = 0.00052g

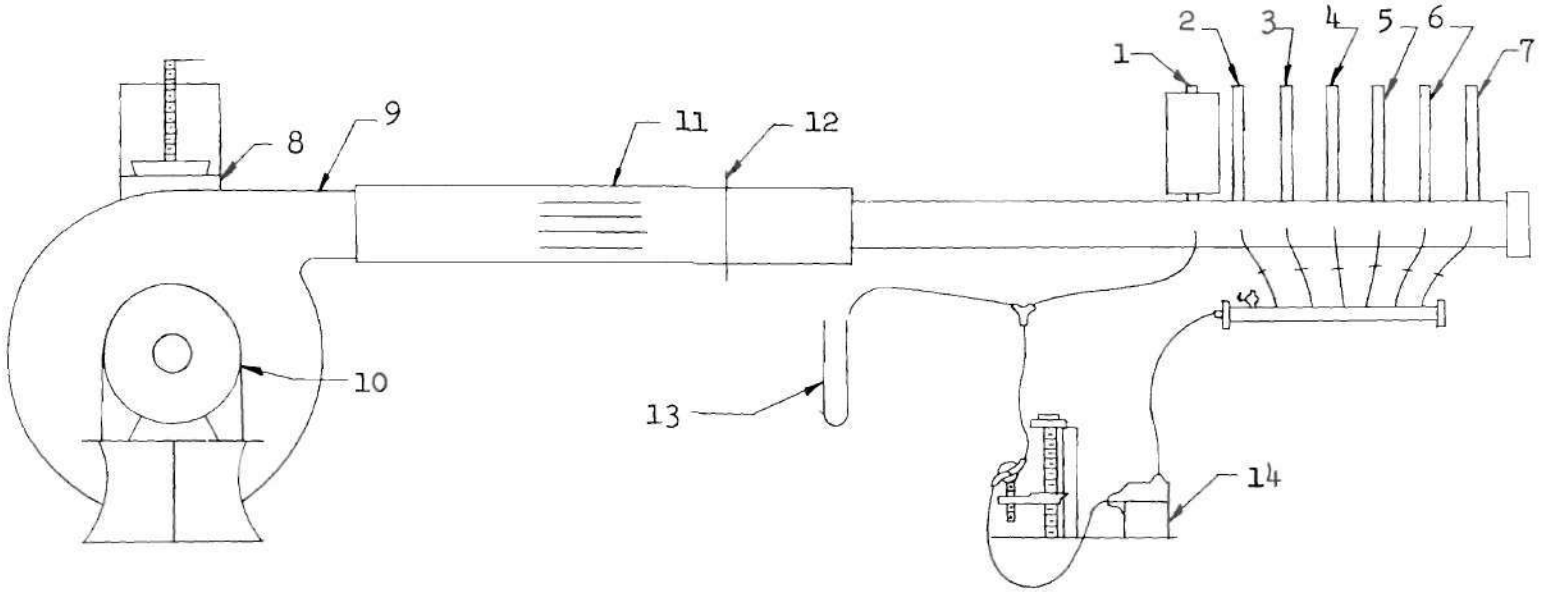

1. Port One
2. Port two
3. Port three
4. Port four
5. Port five
6. Port six
7. Port seven
8. Inlet valve
9. Pressure fan
10. 15 HP motor
11. Straightening vane
12. Orifice
13. "U" tube manometer
14. Micromanometer

Figure 3. Sketch of Test Apparatus

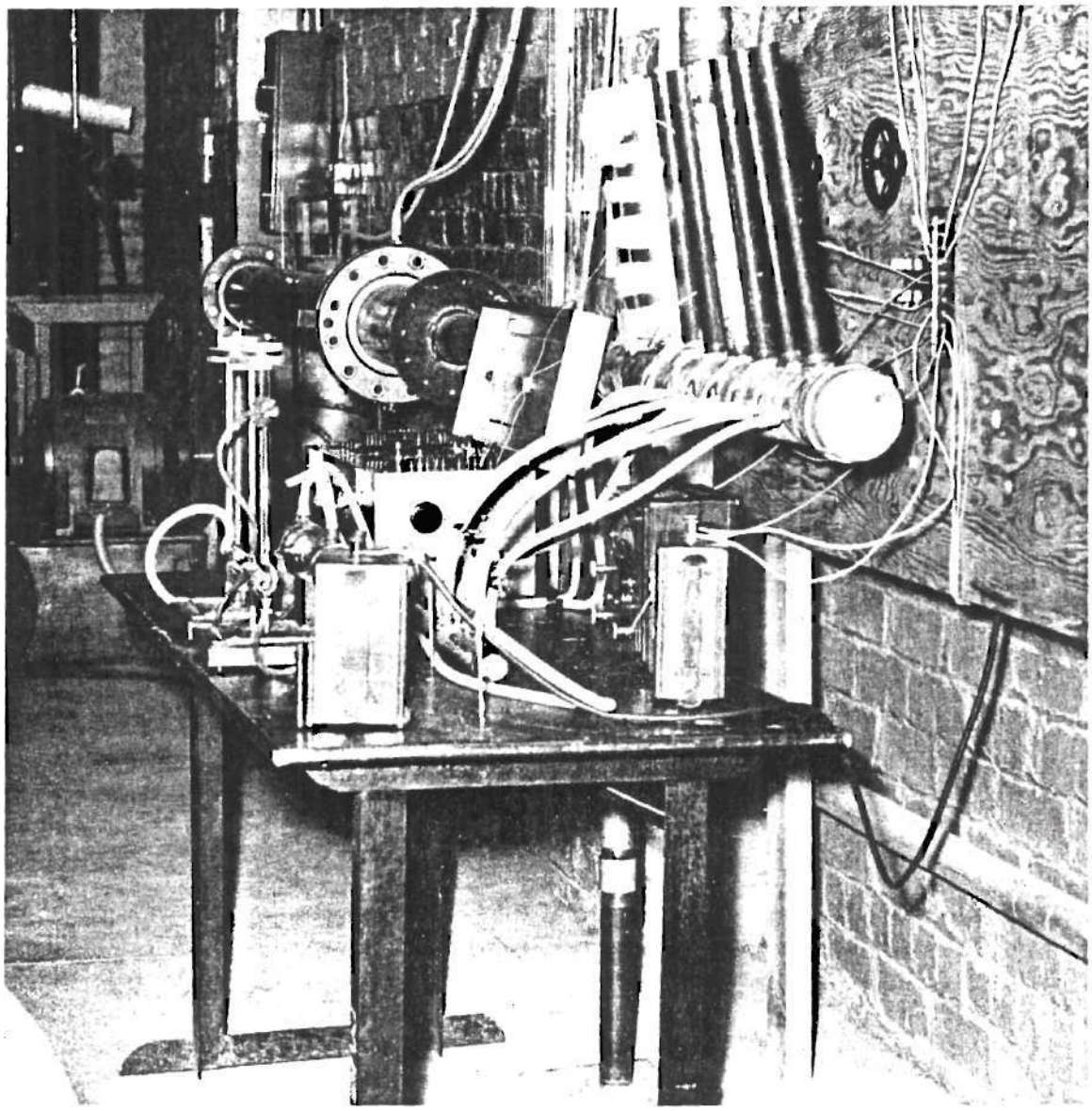

Figure 4. Photograph of Test Apparatus.

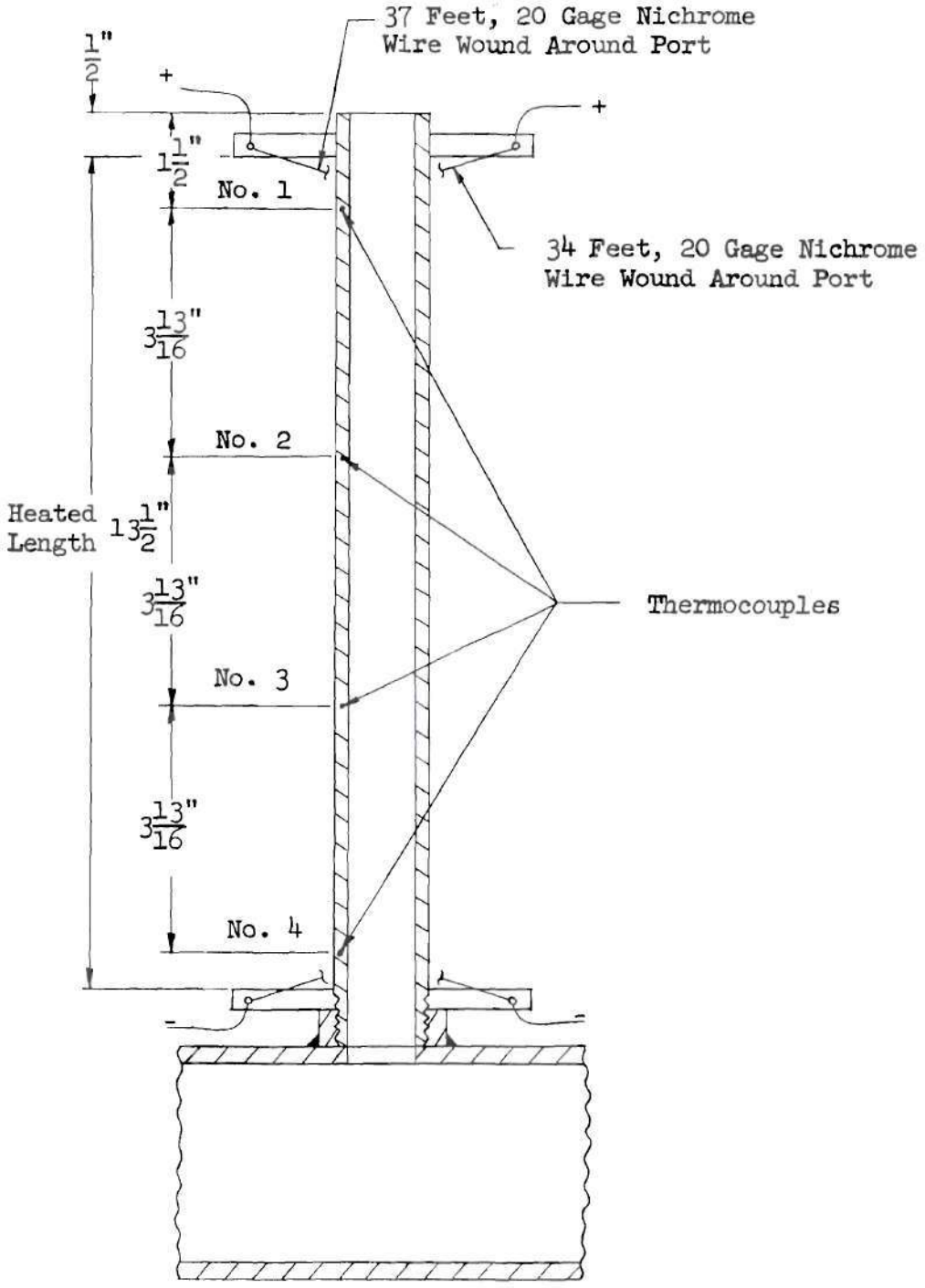

Figure 5. Sketch of Heated Port Assembly

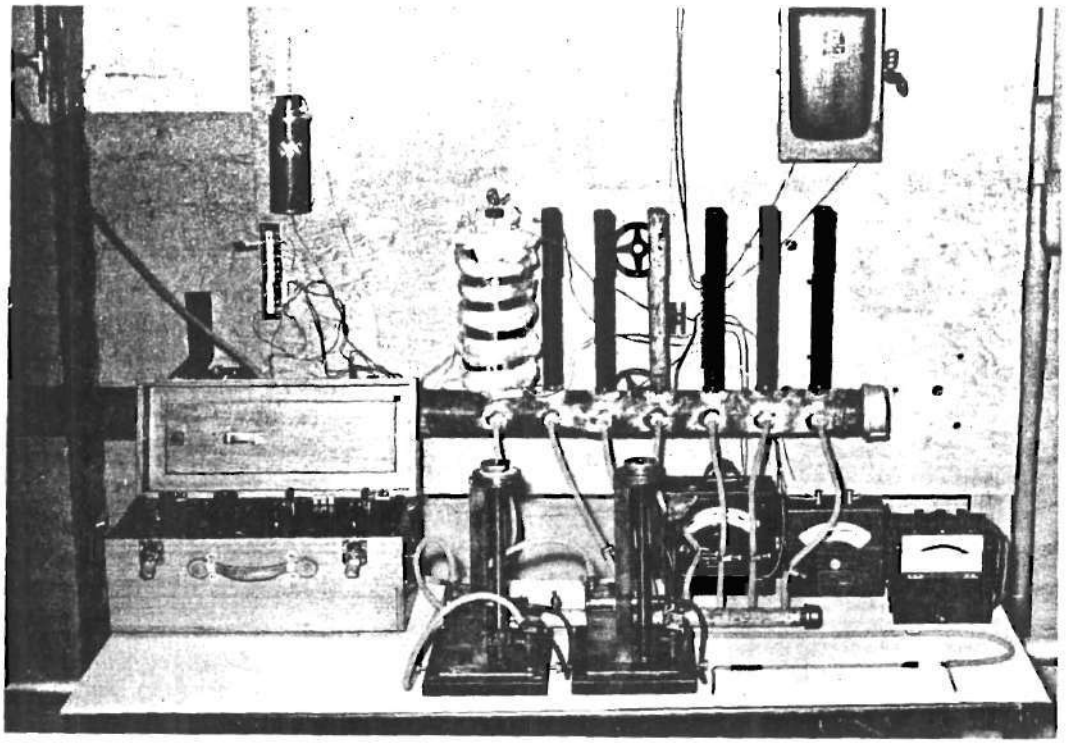

Figure 6. Photograph of Test Section.

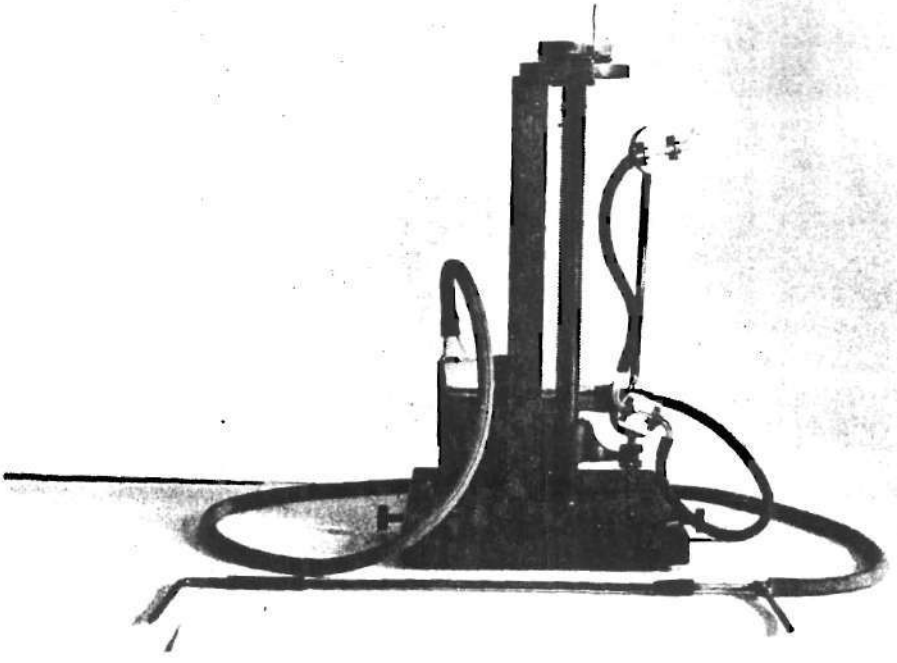

Figure 7. Photograph of Micromanometer to Measure Stagnation Pressure.

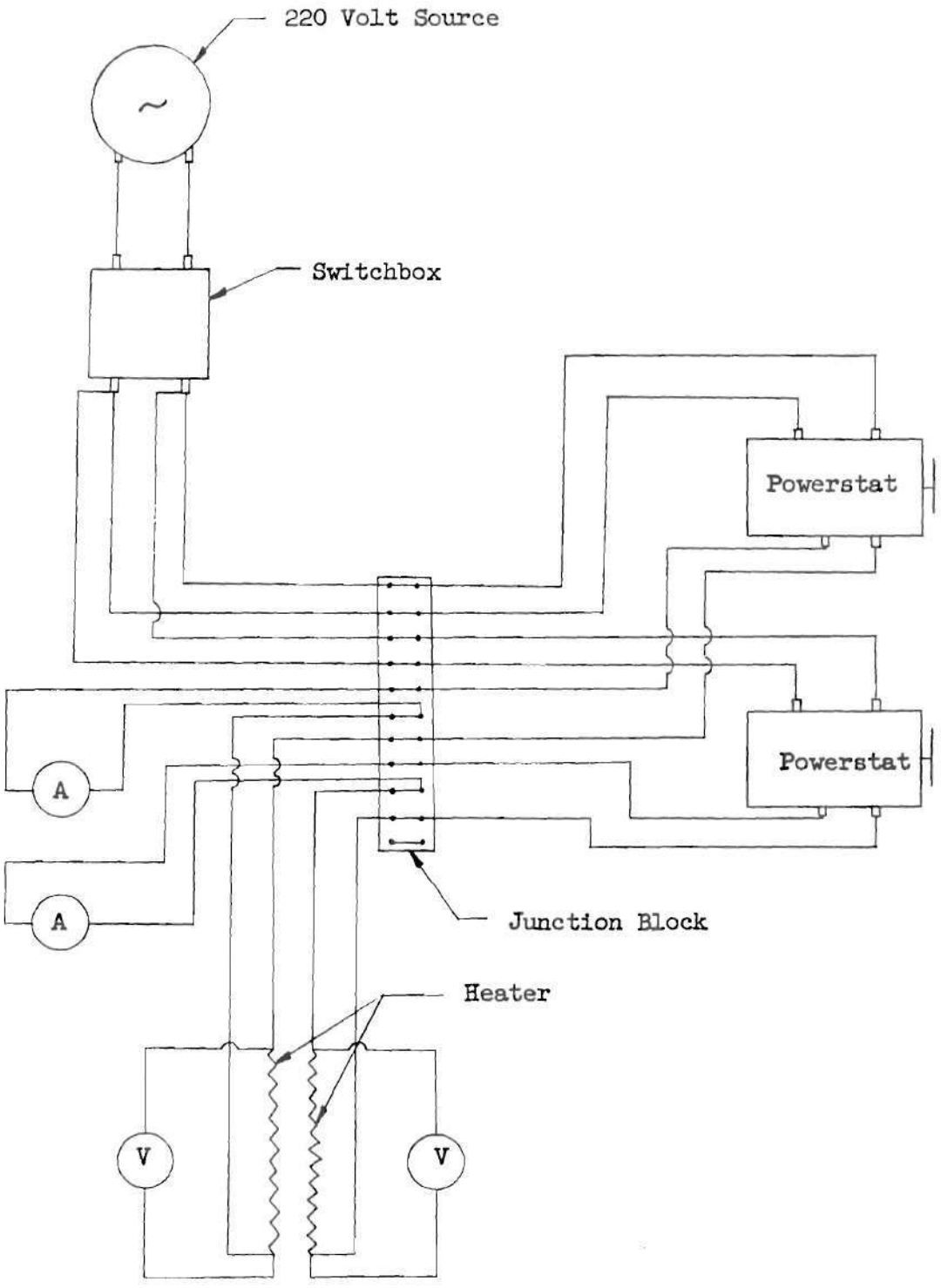

Figure 8. Electrical Heater Circuits

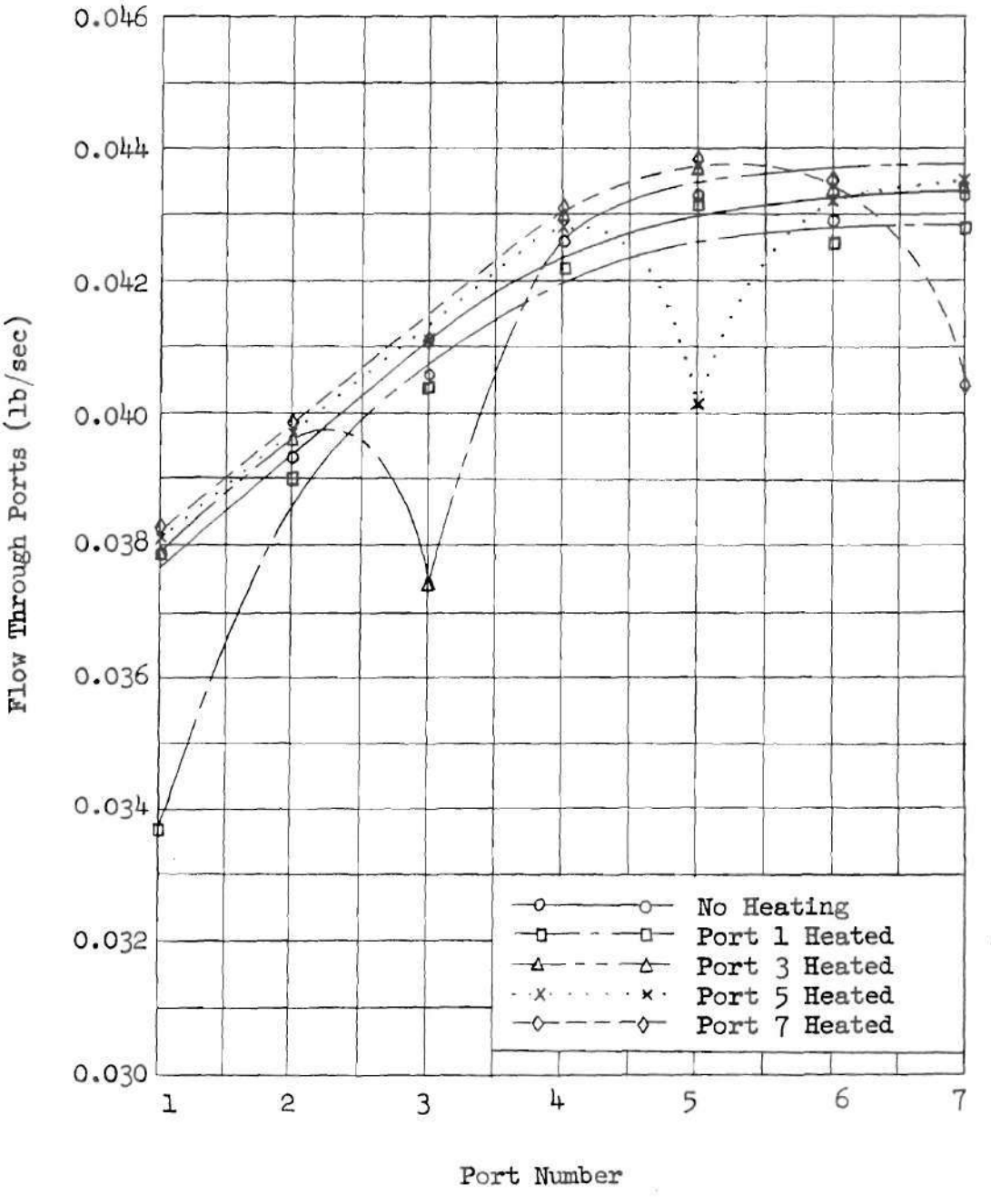

Figure 9. Mass Flow Through Ports For Total Flow of Approximately 0.288 lb/sec

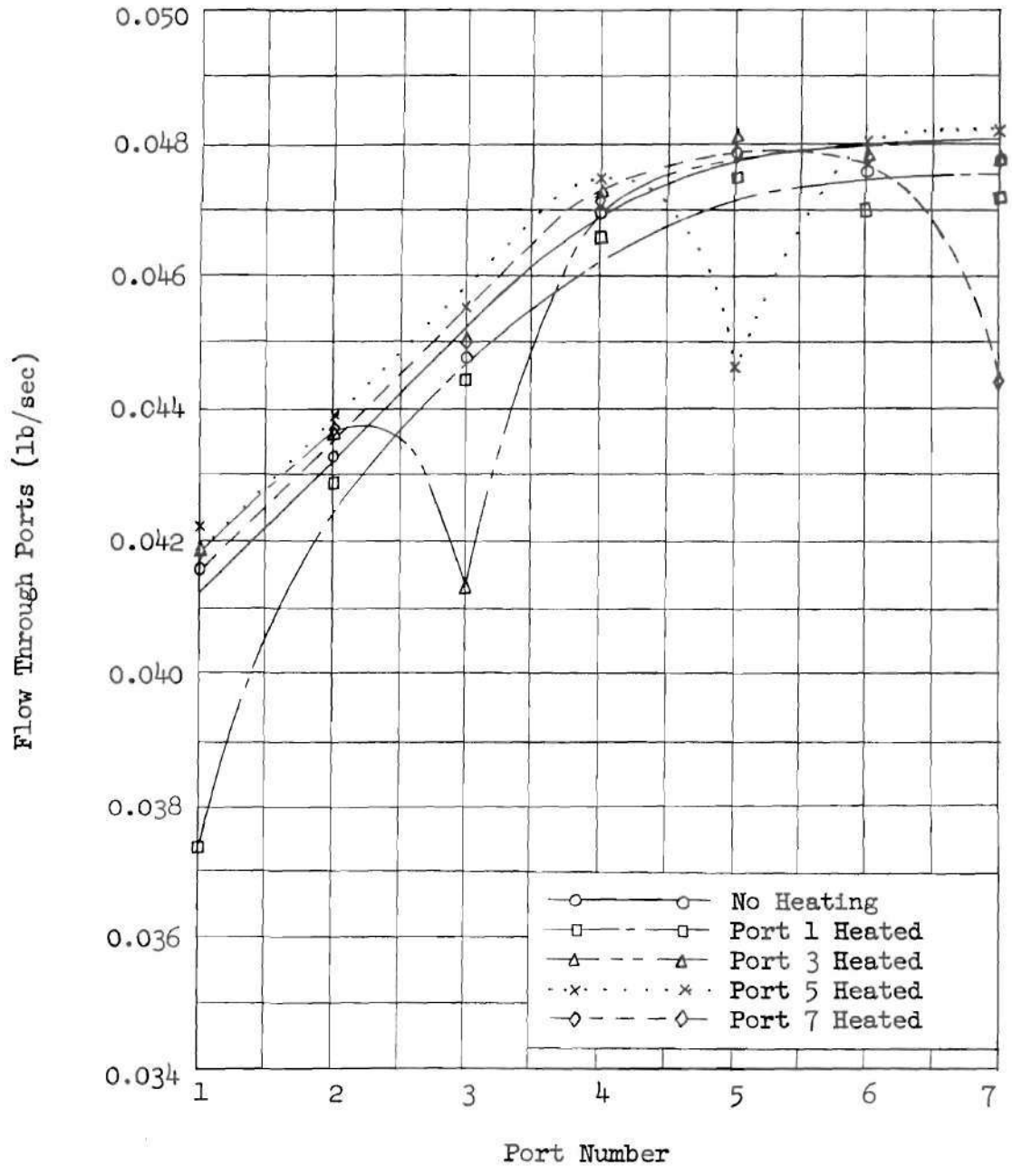

Figure 10. Mass Flow Through Ports For Total Flow of Approximately 0.318 lb/sec

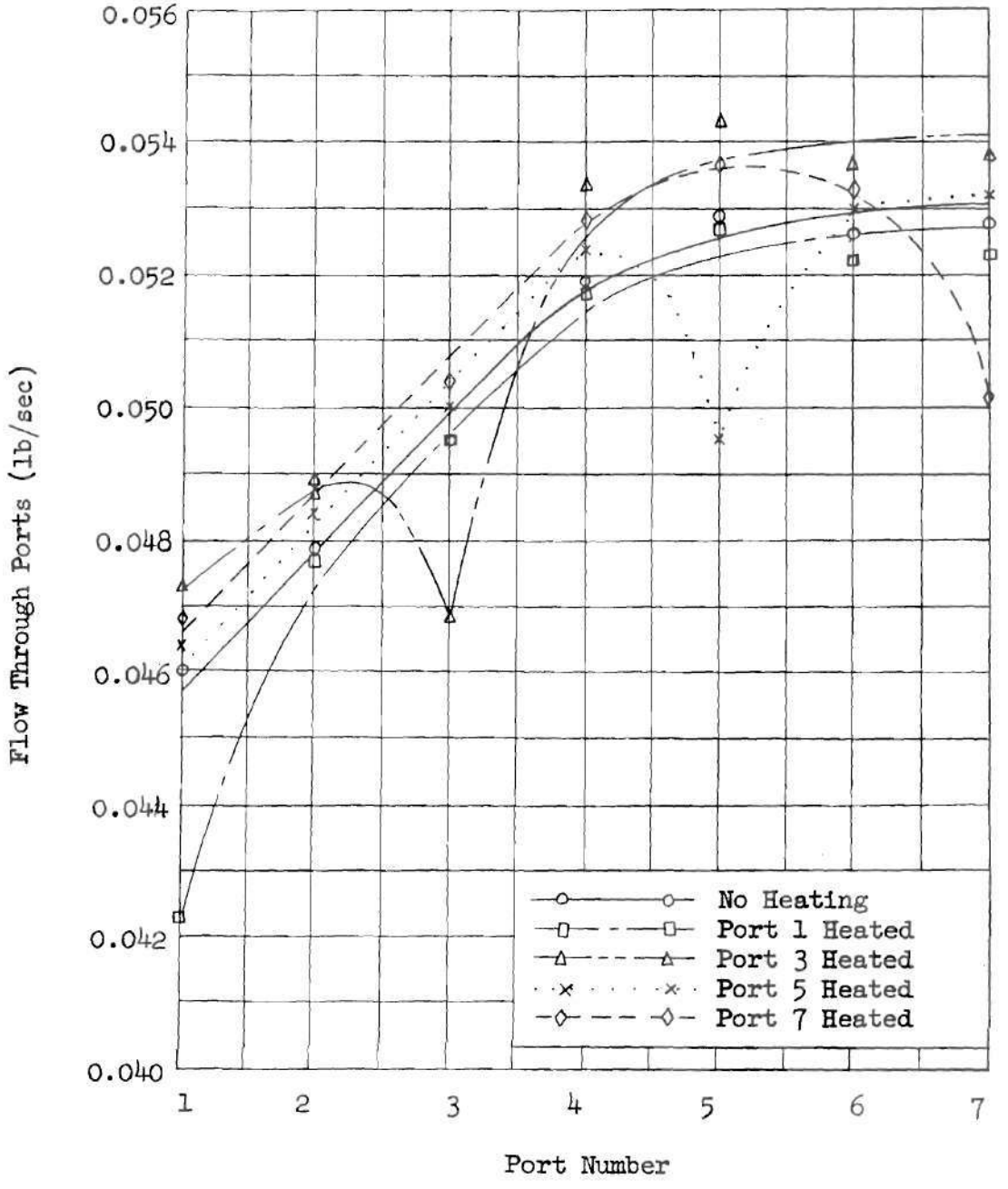

Figure 11. Mass Flow Through Ports For Total Flow of Approximately 0.354 lb/sec

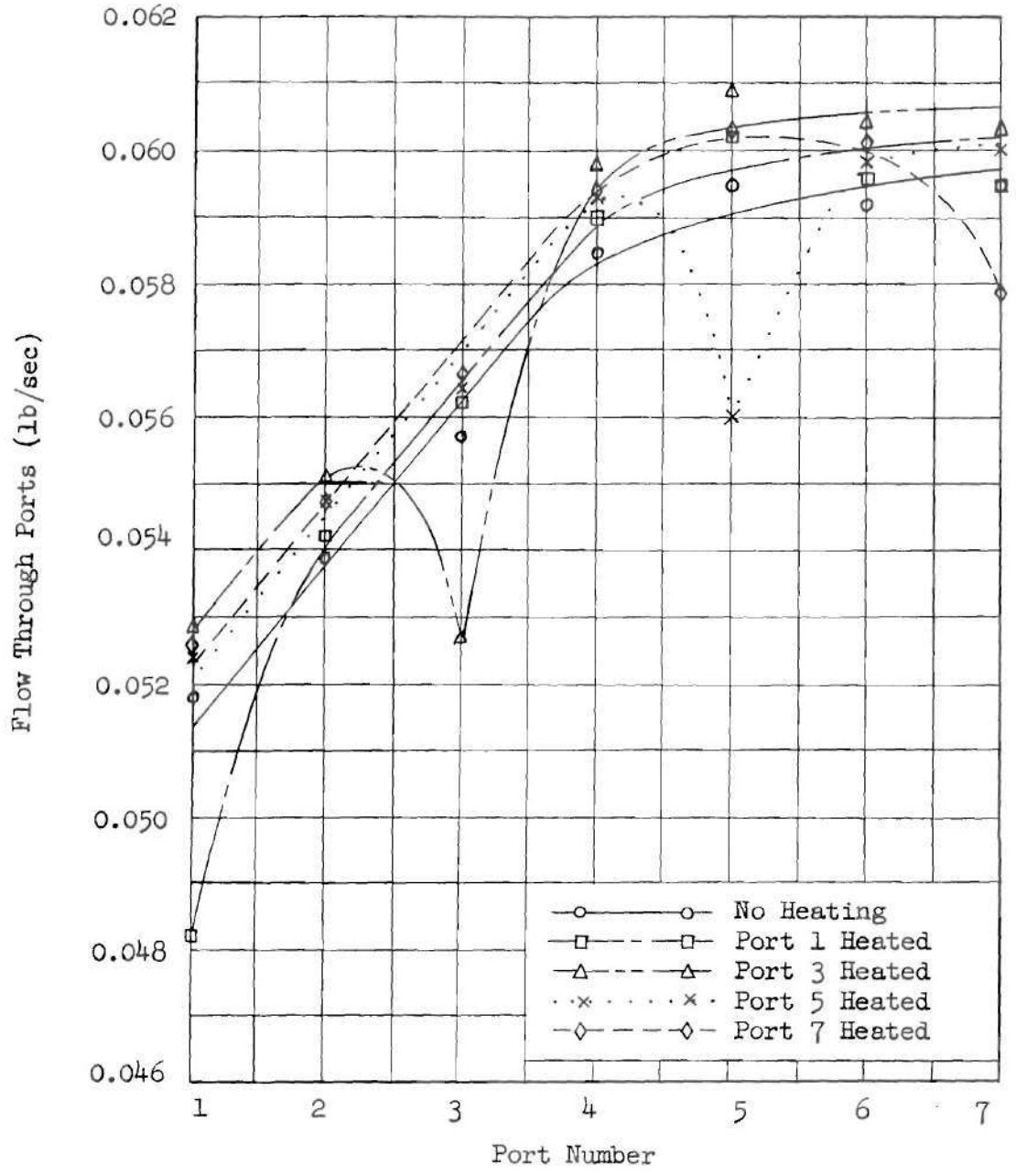

Figure 12. Mass Flow Through Ports For Total Flow of Approximately 0.399 lb/sec

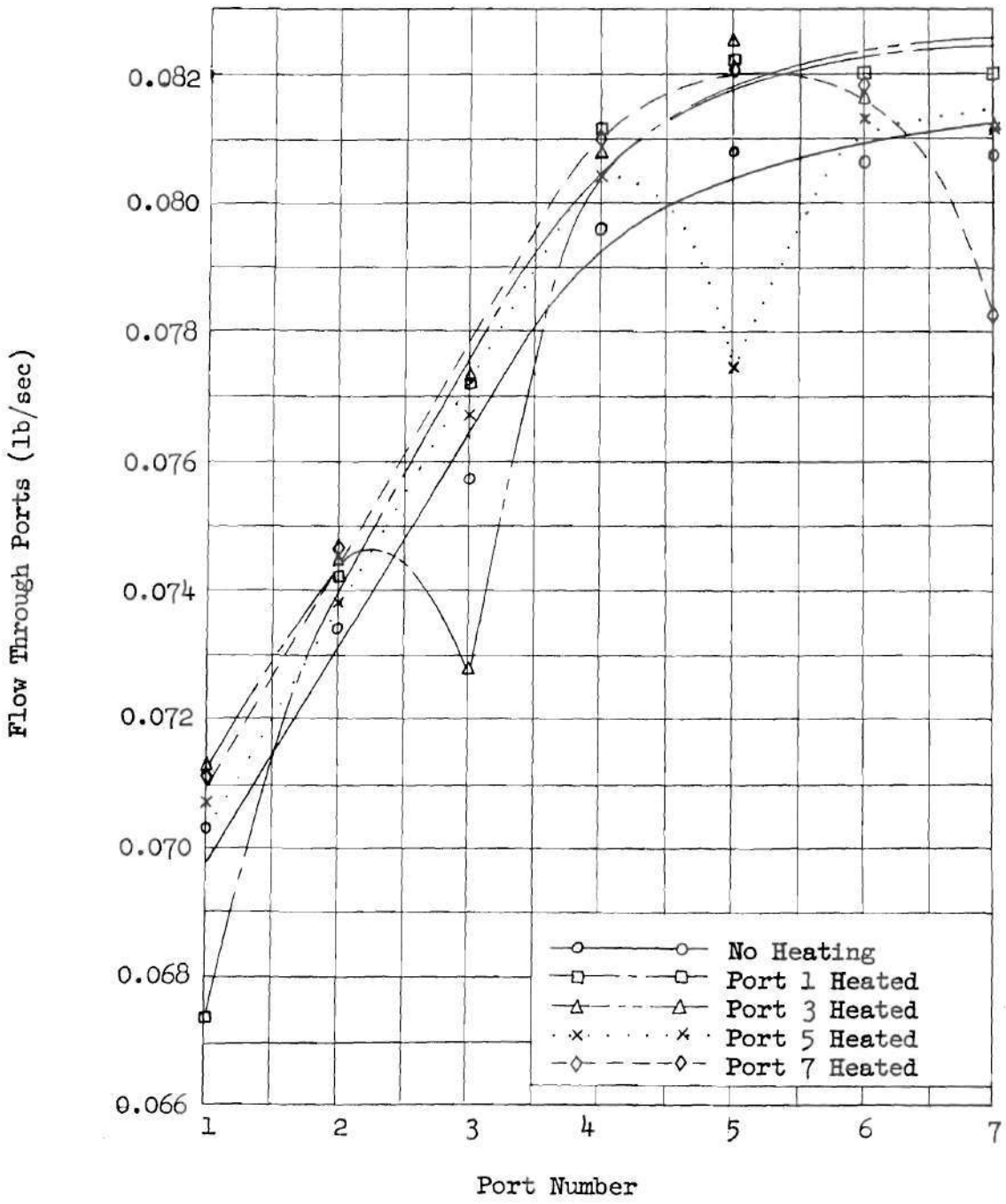

Figure 13. Mass Flow Through Ports For Total Flow of Approximately 0.544 lb/sec

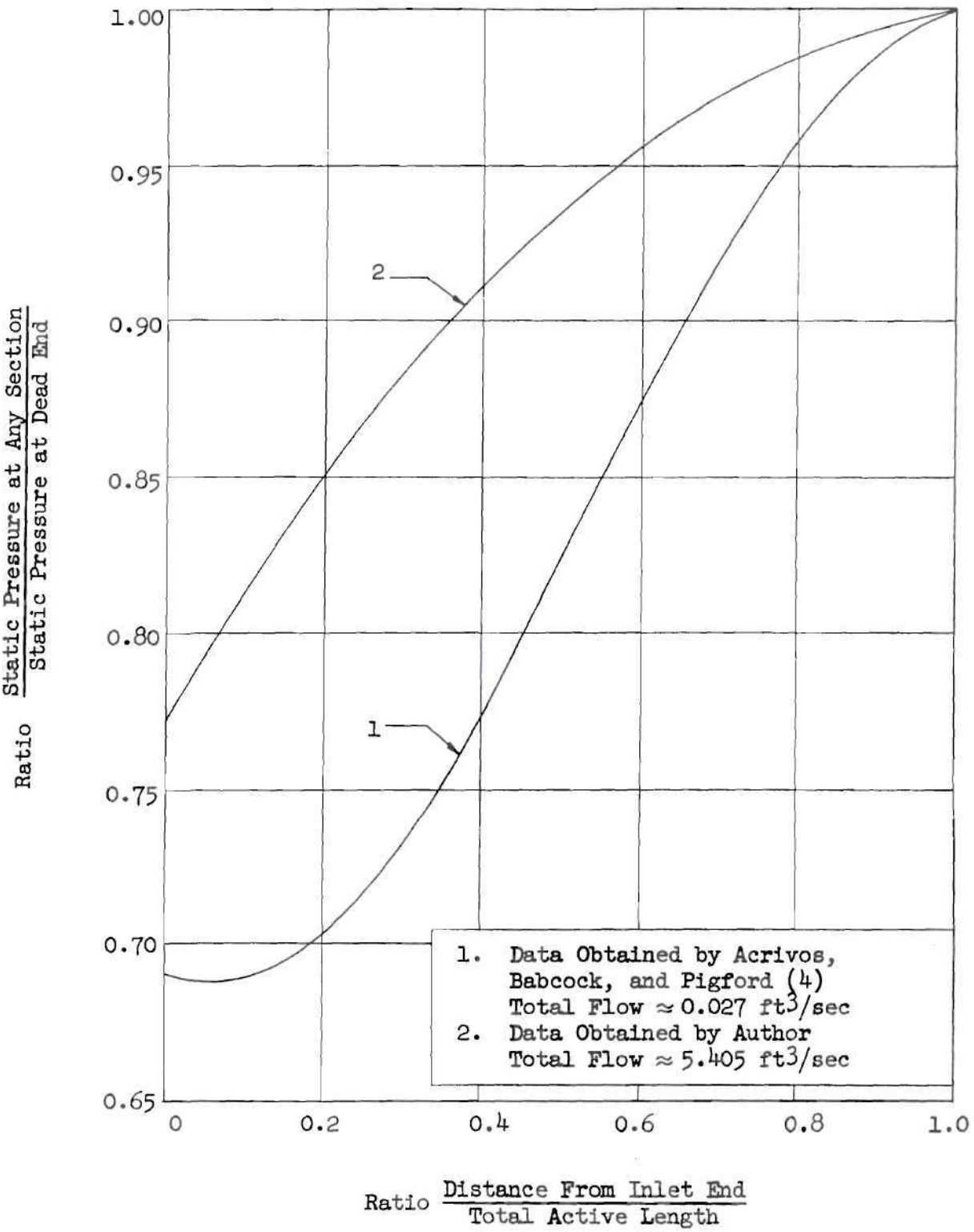

Figure 14. Typical Static Pressure Data Along Manifold Length

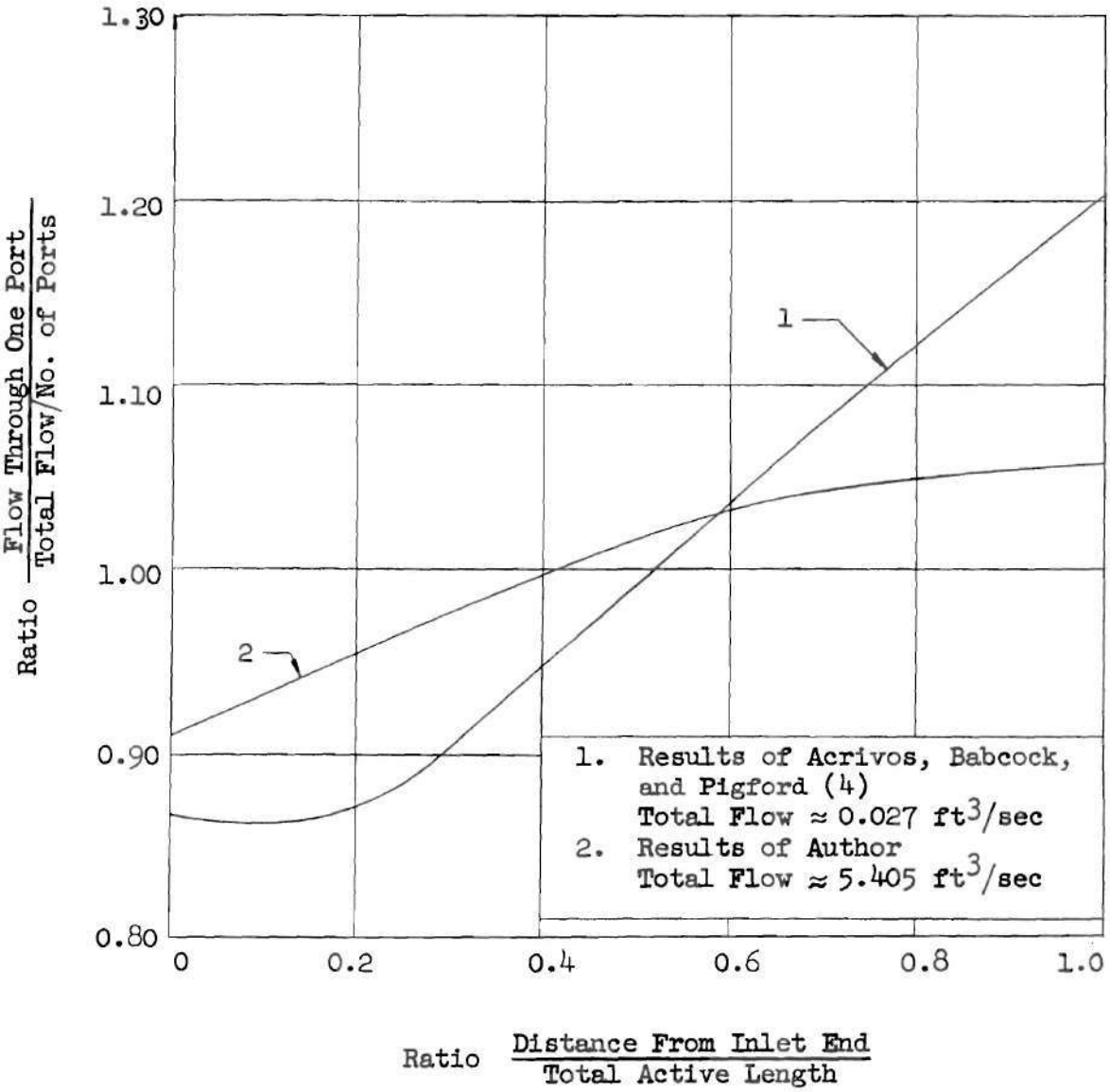

Figure 15. Typical Data of Flow Distribution Through Ports of a Manifold

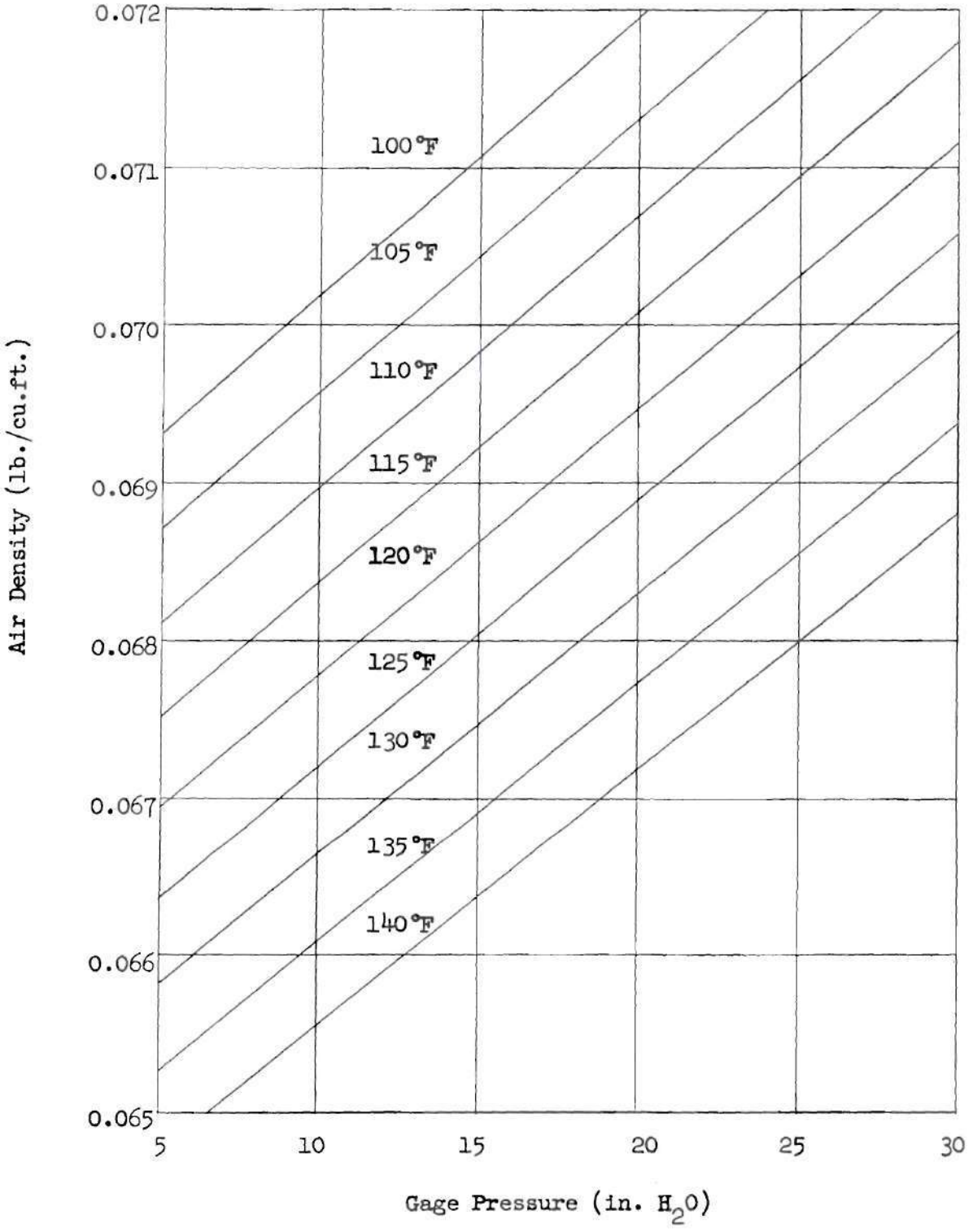

For Barometric Pressure of 28.90 in. Hg. a 0.1 inch Change in Barometric Pressure = 1.36 in. H_2O Change in Gage Pressure.

Figure 16. Air Density Chart

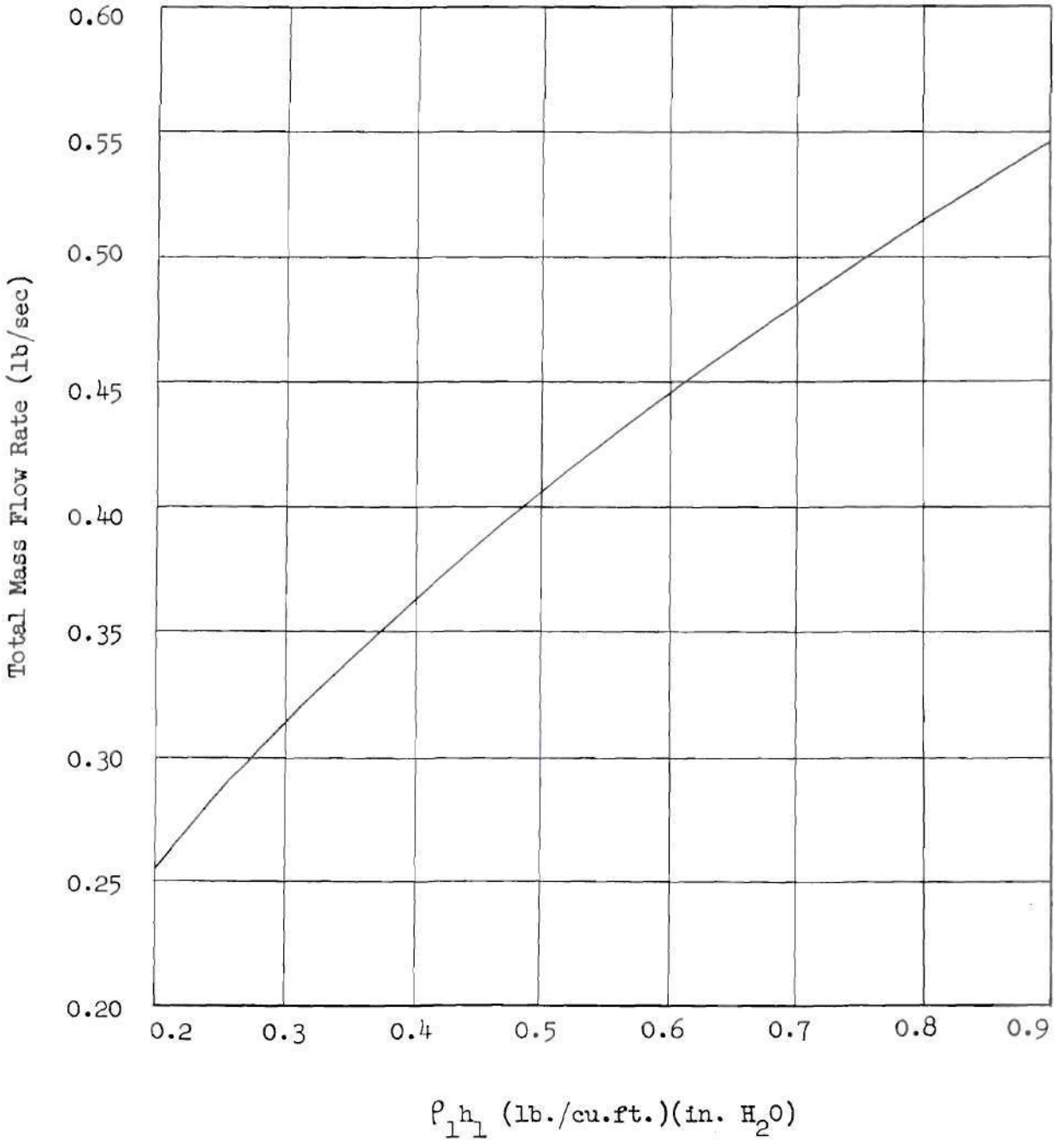

Figure 17. Inlet Orifice Flow Rate

APPENDIX C

TABLES

Table 1. Data For Flow With No Heating

Run No.		1	2	3	4	5
T_o	°F	120	121	135	136	132
h_{s_o}	"H_2O	8.53	10.30	12.80	16.30	29.47
h_1	"H_2O	3.76	4.56	5.64	7.13	12.67
E_{ip}	mv	1.97	2.00	2.16	2.18	2.11
T_{ip}	°F	120	121	128	129	126
h_{s_1}	"H_2O	3.330	4.000	5.030	6.440	11.670
h_{s_2}	"H_2O	3.635	4.323	5.449	6.961	12.663
h_{s_3}	"H_2O	3.886	4.644	5.812	7.433	13.514
h_{s_4}	"H_2O	4.068	4.860	6.079	7.793	14.179
h_{s_5}	"H_2O	4.211	5.025	6.291	8.065	14.664
h_{s_6}	"H_2O	4.297	5.122	6.426	8.238	14.982
h_{s_7}	"H_2O	4.405	5.171	6.502	8.330	15.138
P_{t_1}	"H_2O	2.223	2.668	3.342	4.246	7.768
P_{t_2}	"H_2O	2.393	2.898	3.623	4.601	8.472
P_{t_3}	"H_2O	2.549	3.100	3.861	4.923	9.015
P_{t_4}	"H_2O	2.803	3.413	4.251	5.416	9.960
P_{t_5}	"H_2O	2.901	3.539	4.413	5.612	10.269
P_{t_6}	"H_2O	2.846	3.494	4.360	5.564	10.199
P_{t_7}	"H_2O	2.892	3.524	4.399	5.612	10.225
T_c	°F	120	121	128	129	126
P_b	"Hg	29.00	29.00	29.00	29.00	29.00

Table 2. Data For Flow With Port No. 1 Heated

Run No.		1	2	3	4	5
T_o	°F	135	139	139	136	119
h_{s_o}	"H_2O	8.55	10.43	12.87	16.47	29.47
h_1	"H_2O	3.67	4.48	5.51	7.05	12.67
E_{ip}	mv	2.20	2.27	2.20	2.16	1.99
T_{ip}	°F	130	133	130	128	121
h_{s_1}	"H_2O	3.400	4.130	5.110	6.580	11.800
h_{s_2}	"H_2O	3.744	4.496	5.542	7.141	12.711
h_{s_3}	"H_2O	3.982	4.787	5.931	7.621	13.655
h_{s_4}	"H_2O	4.159	5.024	6.211	8.077	14.324
h_{s_5}	"H_2O	4.300	5.191	6.425	8.261	14.826
h_{s_6}	"H_2O	4.383	5.307	6.566	8.435	15.131
h_{s_7}	"H_2O	4.437	5.375	6.630	8.521	15.279
P_{t_1}	"H_2O	2.283	2.775	3.456	4.408	7.934
P_{t_2}	"H_2O	2.417	2.941	3.663	4.683	8.445
P_{t_3}	"H_2O	2.592	3.153	3.941	5.042	9.119
P_{t_4}	"H_2O	2.839	3.479	4.319	5.552	10.078
P_{t_5}	"H_2O	2.971	3.615	4.480	5.774	10.346
P_{t_6}	"H_2O	2.887	3.541	4.387	5.649	10.285
P_{t_7}	"H_2O	2.912	3.566	4.410	5.641	10.299
T_c	°F	128	132	130	129	121
T_h	°F	282	272	245	240	203
E_1	mv	19.75	17.44	15.55	15.40	11.50
E_2	mv	22.13	20.04	18.02	18.02	14.53
E_3	mv	19.93	17.97	15.83	15.76	11.44
E_4	mv	17.43	15.56	13.92	13.75	10.26
T_1	°F	894	796	716	710	541
T_2	°F	995	907	821	821	672
T_3	°F	902	819	728	725	539
T_4	°F	796	716	646	639	487
P_b	"Hg	29.16	29.16	29.16	29.16	28.88

Table 3. Data For Flow With Port No. 3 Heated

Run No.		1	2	3	4	5
T_o	°F	126	127	126	127	124
h_{s_o}	"H_2O	8.83	10.55	13.17	16.65	29.60
h_1	"H_2O	3.76	4.55	5.70	7.14	12.62
E_{ip}	mv	1.96	2.00	1.97	1.97	1.92
T_{ip}	°F	120	121	120	120	118
h_{s_1}	"H_2O	3.520	4.200	5.310	6.700	11.930
h_{s_2}	"H_2O	3.820	4.523	5.723	7.248	12.930
h_{s_3}	"H_2O	4.056	4.809	6.107	7.704	13.747
h_{s_4}	"H_2O	4.226	5.019	6.366	8.047	14.382
h_{s_5}	"H_2O	4.367	5.194	6.580	8.330	14.891
h_{s_6}	"H_2O	4.449	5.311	6.716	8.501	15.198
h_{s_7}	"H_2O	4.511	5.379	6.797	8.590	15.360
P_{t_1}	"H_2O	2.315	2.793	3.500	4.425	7.875
P_{t_2}	"H_2O	2.530	3.025	3.705	4.805	8.607
P_{t_3}	"H_2O	2.697	3.217	4.048	5.121	9.211
P_{t_4}	"H_2O	2.983	3.560	4.465	5.648	10.148
P_{t_5}	"H_2O	3.075	3.686	4.611	5.868	10.566
P_{t_6}	"H_2O	3.038	3.631	4.525	5.776	10.333
P_{t_7}	"H_2O	3.040	3.638	4.528	5.760	10.232
T_c	°F	116	119	119	120	118
T_h	°F	227	224	218	214	188
E_1	mv	15.30	15.29	14.40	13.65	11.27
E_2	mv	19.25	19.01	17.93	17.04	13.95
E_3	mv	15.40	15.25	14.36	13.64	11.26
E_4	mv	13.75	13.70	12.56	11.56	8.79
T_1	°F	705	705	667	634	531
T_2	°F	873	863	817	779	647
T_3	°F	710	703	665	634	531
T_4	°F	639	637	586	544	422
P_b	"Hg.	28.93	28.93	28.93	28.93	28.93

Table 4. Data For Flow With Port No. 5 Heated

Run No.		1	2	3	4	5
T_o	°F	130	124	133	132	130
h_{s_o}	"H_2O	8.78	10.51	13.00	16.57	29.55
h_1	"H_2O	3.77	4.58	5.62	7.12	12.63
E_{ip}	mv	2.05	2.04	2.10	2.08	2.04
T_{ip}	°F	124	123	125	125	123
h_{s_1}	"H_2O	3.530	4.210	5.230	6.670	11.900
h_{s_2}	"H_2O	3.805	4.580	5.660	7.241	12.905
h_{s_3}	"H_2O	4.053	4.877	6.036	7.704	13.741
h_{s_4}	"H_2O	4.251	5.101	6.299	8.070	14.401
h_{s_5}	"H_2O	4.384	5.266	6.510	8.328	14.892
h_{s_6}	"H_2O	4.470	5.349	6.641	8.485	15.193
h_{s_7}	"H_2O	4.549	5.417	6.745	8.579	15.341
P_{t_1}	"H_2O	2.323	2.787	3.453	4.410	7.814
P_{t_2}	"H_2O	2.529	3.017	3.758	4.806	8.511
P_{t_3}	"H_2O	2.706	3.250	4.001	5.122	9.174
P_{t_4}	"H_2O	2.935	3.544	4.409	5.645	10.094
P_{t_5}	"H_2O	3.026	3.676	4.571	5.838	10.475
P_{t_6}	"H_2O	2.992	3.608	4.500	5.753	10.307
P_{t_7}	"H_2O	3.030	3.642	4.533	5.785	10.268
T_c	°F	123	123	126	125	123
T_h	°F	224	227	221	218	192
E_1	mv	14.20	15.03	14.35	13.40	11.00
E_2	mv	17.65	18.79	17.80	16.65	13.76
E_3	mv	14.80	15.52	14.73	13.73	11.24
E_4	mv	13.05	13.56	12.93	12.07	9.97
T_1	°F	658	694	665	624	519
T_2	°F	805	854	812	763	639
T_3	°F	684	715	681	638	530
T_4	°F	609	631	603	566	474
P_b	"Hg	29.05	29.00	29.00	29.00	29.00

Table 5. Data For Flow With Port No. 7 Heated

Run No.		1	2	3	4	5
T_o	°F	120	132	133	124	118
h_{s_o}	"H_2O	8.60	10.59	13.16	16.46	29.45
h_1	"H_2O	3.76	4.58	5.70	7.11	12.65
E_{ip}	mv	1.98	2.11	2.11	2.00	1.97
T_{ip}	°F	120	126	126	121	120
h_{s_1}	"H_2O	3.430	4.250	5.260	6.560	11.780
h_{s_2}	"H_2O	3.735	4.592	5.706	7.056	12.682
h_{s_3}	"H_2O	3.982	4.887	6.077	7.552	13.641
h_{s_4}	"H_2O	4.155	5.112	6.351	7.895	14.283
h_{s_5}	"H_2O	4.291	5.284	6.553	8.163	14.762
h_{s_6}	"H_2O	4.353	5.391	6.679	8.324	15.038
h_{s_7}	"H_2O	4.410	5.479	6.758	8.410	15.181
P_{t_1}	"H_2O	2.296	2.817	3.496	4.344	7.751
P_{t_2}	"H_2O	2.490	3.069	3.811	4.708	8.514
P_{t_3}	"H_2O	2.646	3.258	4.059	5.041	9.144
P_{t_4}	"H_2O	2.905	3.577	4.459	5.544	10.049
P_{t_5}	"H_2O	3.006	3.689	4.600	5.718	10.324
P_{t_6}	"H_2O	2.957	3.676	4.545	5.682	10.249
P_{t_7}	"H_2O	3.052	3.808	4.687	5.841	10.535
T_c	°F	120	124	124	121	120
T_h	°F	231	242	224	184	190
E_1	mv	16.02	16.59	13.97	10.24	11.16
E_2	mv	20.14	21.00	19.10	13.08	14.09
E_3	mv	16.94	17.72	15.73	10.55	11.61
E_4	mv	14.46	14.81	12.66	8.71	9.45
T_1	°F	736	760	648	486	526
T_2	°F	911	947	867	610	653
T_3	°F	775	808	724	499	546
T_4	°F	669	684	592	418	451
P_b	"Hg	29.03	29.03	29.03	28.95	28.90

Table 6. Calculated Results For No Heating

Run No.	Port No.	ρ lb/ft^3	U ft/sec	$\bar{u}$ ft/sec	W_p lb/sec
1	1	0.0663	106.0	92.0	0.0379
	2	0.0663	110.0	95.5	0.0394
	3	0.0663	113.5	98.5	0.0406
	4	0.0663	119.0	103.3	0.0426
	5	0.0663	121.1	105.1	0.0433
	6	0.0663	119.9	104.1	0.0429
	7	0.0663	120.9	104.9	0.0433
2	1	0.0662	116.2	101.0	0.0416
	2	0.0662	121.1	105.2	0.0433
	3	0.0662	125.3	108.9	0.0448
	4	0.0662	131.4	114.2	0.0470
	5	0.0662	133.8	116.3	0.0479
	6	0.0662	133.0	115.6	0.0476
	7	0.0662	133.6	116.1	0.0478
3	1	0.0654	130.9	113.1	0.0460
	2	0.0654	136.3	117.8	0.0479
	3	0.0654	140.7	121.6	0.0495
	4	0.0654	147.6	127.5	0.0519
	5	0.0654	150.4	129.9	0.0529
	6	0.0654	149.5	129.2	0.0526
	7	0.0654	150.1	129.7	0.0528
4	1	0.0653	147.6	127.4	0.0518
	2	0.0653	153.7	132.6	0.0539
	3	0.0653	159.0	137.2	0.0557
	4	0.0653	166.7	143.9	0.0585
	5	0.0653	169.7	146.5	0.0595
	6	0.0653	169.0	145.8	0.0592
	7	0.0653	169.7	146.5	0.0595
5	1	0.0656	199.2	172.3	0.0703
	2	0.0656	208.0	179.9	0.0734
	3	0.0656	214.6	185.6	0.0757
	4	0.0656	225.6	195.1	0.0796
	5	0.0656	229.0	198.1	0.0808
	6	0.0656	228.3	197.5	0.0806
	7	0.0656	228.6	197.7	0.0807

Table 7. Calculated Results For Port No. 1 Heated

Run No.	Port No.	ρ lb/ft^3	U ft/sec	$\bar{u}$ ft/sec	W_p lb/sec
1	1	0.0521	121.2	104.0	0.0337
	2	0.0658	111.0	95.2	0.0390
	3	0.0658	114.9	98.6	0.0404
	4	0.0658	120.2	103.1	0.0422
	5	0.0658	123.0	105.5	0.0432
	6	0.0658	121.3	104.1	0.0426
	7	0.0658	121.8	104.5	0.0428
2	1	0.0528	132.7	114.0	0.0374
	2	0.0653	122.9	105.6	0.0429
	3	0.0653	127.2	109.3	0.0444
	4	0.0653	133.6	114.8	0.0466
	5	0.0653	136.2	117.0	0.0475
	6	0.0653	134.8	115.8	0.0470
	7	0.0653	135.3	116.2	0.0472
3	1	0.0549	145.2	124.0	0.0423
	2	0.0656	136.8	116.8	0.0477
	3	0.0656	141.9	121.2	0.0495
	4	0.0656	148.5	126.8	0.0517
	5	0.0656	151.3	129.2	0.0527
	6	0.0656	149.7	127.8	0.0522
	7	0.0656	150.0	128.1	0.0523
4	1	0.0553	163.4	140.2	0.0482
	2	0.0657	154.6	132.6	0.0542
	3	0.0657	160.4	137.6	0.0562
	4	0.0657	168.3	144.4	0.0590
	5	0.0657	171.6	147.2	0.0602
	6	0.0657	169.8	145.7	0.0596
	7	0.0657	169.6	145.5	0.0595
5	1	0.0578	214.5	187.5	0.0674
	2	0.0659	207.2	181.1	0.0742
	3	0.0659	215.3	188.2	0.0772
	4	0.0659	226.4	197.9	0.0811
	5	0.0659	229.4	200.5	0.0822
	6	0.0659	228.7	199.9	0.0820
	7	0.0659	228.9	200.1	0.0820

Table 8. Calculated Results For Port No. 3 Heated

Run No.	Port No.	ρ lb/ft^3	U ft/sec	$\bar{u}$ ft/sec	W_p lb/sec
1	1	0.0666	107.9	91.4	0.0379
	2	0.0666	112.8	95.5	0.0396
	3	0.0559	127.2	107.7	0.0374
	4	0.0666	122.5	103.8	0.0430
	5	0.0666	124.4	105.4	0.0437
	6	0.0666	123.6	104.7	0.0434
	7	0.0666	123.7	104.8	0.0434
2	1	0.0663	118.8	101.6	0.0419
	2	0.0663	123.7	105.8	0.0436
	3	0.0561	138.6	118.5	0.0413
	4	0.0663	134.1	114.7	0.0473
	5	0.0663	136.5	116.7	0.0481
	6	0.0663	135.5	115.9	0.0478
	7	0.0663	135.6	115.9	0.0478
3	1	0.0663	133.0	114.6	0.0473
	2	0.0663	136.9	118.0	0.0487
	3	0.0566	154.8	133.4	0.0469
	4	0.0663	150.2	129.5	0.0534
	5	0.0663	152.7	131.6	0.0543
	6	0.0663	151.2	130.3	0.0537
	7	0.0663	151.3	130.4	0.0538
4	1	0.0662	149.7	128.4	0.0529
	2	0.0662	156.0	133.8	0.0551
	3	0.0569	173.7	149.0	0.0527
	4	0.0662	169.1	145.1	0.0598
	5	0.0662	172.4	147.9	0.0609
	6	0.0662	171.0	146.7	0.0604
	7	0.0662	170.8	146.5	0.0603
5	1	0.0664	199.4	172.5	0.0713
	2	0.0664	208.4	180.3	0.0745
	3	0.0592	228.4	197.6	0.0728
	4	0.0664	226.3	195.7	0.0808
	5	0.0664	230.9	199.7	0.0825
	6	0.0664	228.4	197.6	0.0816
	7	0.0664	227.3	196.6	0.0812

Table 9. Calculated Results For Port No. 5 Heated

Run No.	Port No.	ρ lb/ft^3	U ft/sec	$\bar{u}$ ft/sec	W_p lb/sec
1	1	0.0661	108.5	92.6	0.0381
	2	0.0661	113.2	96.6	0.0397
	3	0.0661	117.1	99.9	0.0411
	4	0.0661	122.0	104.1	0.0428
	5	0.0563	134.2	114.5	0.0401
	6	0.0661	123.2	105.1	0.0432
	7	0.0661	123.9	105.7	0.0435
2	1	0.0660	119.0	102.7	0.0422
	2	0.0660	123.8	106.8	0.0439
	3	0.0660	128.5	110.9	0.0455
	4	0.0660	134.1	115.7	0.0475
	5	0.0560	148.3	128.0	0.0446
	6	0.0660	135.4	116.9	0.0480
	7	0.0660	136.0	117.4	0.0482
3	1	0.0656	132.8	113.7	0.0464
	2	0.0656	138.6	118.6	0.0484
	3	0.0656	143.0	122.4	0.0500
	4	0.0656	150.1	128.5	0.0524
	5	0.0565	164.7	141.0	0.0495
	6	0.0656	151.6	129.8	0.0530
	7	0.0656	152.2	130.3	0.0532
4	1	0.0658	149.9	128.0	0.0524
	2	0.0658	156.5	133.7	0.0547
	3	0.0658	161.5	137.9	0.0564
	4	0.0658	169.6	144.8	0.0593
	5	0.0567	185.8	158.7	0.0560
	6	0.0658	171.2	146.2	0.0598
	7	0.0658	171.7	146.6	0.0600
5	1	0.0660	199.2	172.3	0.0707
	2	0.0660	207.9	179.8	0.0738
	3	0.0660	215.8	186.7	0.0767
	4	0.0660	226.4	195.8	0.0804
	5	0.0590	243.9	211.0	0.0774
	6	0.0660	228.8	197.9	0.0813
	7	0.0660	228.3	197.5	0.0811

Table 10. Calculated Results For Port No. 7 Heated

Run No.	Port No.	ρ lb/ft^3	U ft/sec	$\bar{u}$ ft/sec	W_p lb/sec
1	1	0.0664	107.6	92.6	0.0383
	2	0.0664	112.1	96.5	0.0399
	3	0.0664	115.6	99.5	0.0411
	4	0.0664	121.1	104.3	0.0431
	5	0.0664	123.2	106.1	0.0438
	6	0.0664	122.2	105.2	0.0435
	7	0.0557	135.5	116.7	0.0404
2	1	0.0659	119.7	102.1	0.0419
	2	0.0659	124.9	106.5	0.0437
	3	0.0659	128.7	109.8	0.0450
	4	0.0659	134.9	115.1	0.0472
	5	0.0659	137.0	116.9	0.0479
	6	0.0659	136.7	116.6	0.0478
	7	0.0549	152.5	130.1	0.0444
3	1	0.0659	133.3	114.1	0.0468
	2	0.0659	139.2	119.2	0.0489
	3	0.0659	143.7	123.0	0.0504
	4	0.0659	150.6	128.9	0.0528
	5	0.0659	152.9	130.9	0.0537
	6	0.0659	152.0	130.1	0.0533
	7	0.0563	167.0	143.0	0.0501
4	1	0.0661	148.4	127.8	0.0526
	2	0.0661	154.5	133.0	0.0547
	3	0.0661	159.9	137.7	0.0566
	4	0.0661	167.7	144.4	0.0594
	5	0.0661	170.3	146.6	0.0603
	6	0.0661	169.7	146.1	0.0601
	7	0.0596	181.2	156.0	0.0578
5	1	0.0661	198.2	173.0	0.0711
	2	0.0661	207.8	181.4	0.0746
	3	0.0661	215.3	188.0	0.0773
	4	0.0661	225.7	197.0	0.0810
	5	0.0661	228.8	199.7	0.0821
	6	0.0661	228.0	199.0	0.0818
	7	0.0590	244.6	213.5	0.0783

APPENDIX D

DETERMINATION OF AIR FLOW RESULTS

Determination of inlet air flow.--The orifice meter used to measure the inlet air was constructed by the Foxboro Company in accordance with the specifications for thin plate orifices given in the A.S.M.E. Research Committee Report on Fluid Meters. (9) Standard flange pressure taps were used with the taps being located one inch upstream and one inch downstream from the orifice plate.

The flow equation for the thin plate orifice is

$$W_t = 0.0997 \frac{C}{\sqrt{1 - \gamma^4}} D_2^2 \sqrt{\rho_1 h_1}$$

where

W_t = mass flow rate, lb/sec

C = coefficient of discharge

D_2 = orifice diameter, in.

$\gamma = D_2/D_1 = 0.5$

D_1 = pipe diameter, in.

ρ_1 = upstream air density, lb/cu.ft.

h_1 = orifice pressure differential, in. H_2O

The Fluid Meters Report gives experimentally determined values for the expression

$$\frac{C}{\sqrt{1 - \gamma^4}} = K_1$$

based on the pipe size and the Reynolds number. It was estimated that the mass flow rate would be between 0.3 lb/sec and 0.6 lb/sec and the resulting Reynolds numbers were from 65,000 to 125,000. For this range of Reynolds numbers and for the pipe size and D_2/D_1 ratio used the value for K_1 was given as 0.6276.

Two curves were plotted to facilitate the solution of the flow equation. The first of these, Figure 16, was a plot of air density, ρ_1, versus static pressure in inches of water with the temperature as the parameter. A barometric pressure of 28.90 in.Hg. was used in the construction of the curve and any variation from this was accounted for by adjusting the static pressure. The density is given by the expression

$$\rho_1 = \frac{2044.1 + 5.2\ h_{s_o}}{RT_o}$$

where

h_{s_o} = upstream static pressure, gage, inlet air orifice, in.H_2O

R = the gas constant for air, 53.3

T_o = upstream temperature, inlet air orifice, degrees Rankine

The second curve, Figure 17, is a plot of mass flow, W_t, versus the product, $\rho_1 h_1$. By the use of these two curves the mass flow rate through the inlet air orifice could be determined rapidly and with an accuracy of three significant figures.

Determination of air flow through ports.--The center line velocity at the exit of each port was computed by the equation

$$U = \sqrt{\frac{2\beta (P_t - P_s)}{\rho}}$$

where

U = center line velocity at exit of port, ft/sec

β = dimensional constant 32.2 $lb_m ft/lb_f\ sec^2$

P_t = stagnation pressure at exit of port, lb/ft^2

P_s = static pressure at exit of port, lb/ft^2

ρ = density of fluid at exit of port, lb/ft^3

With the total flow rate and center line velocity known, it was then possible to determine the average velocity out of each port. The equation to solve for the average velocity out of each port is

$$\bar{u} = aU$$

where

$\bar{u}$ = average velocity, ft/sec

a = constant

The constant, a, is determined by the expression

$$a = \frac{W_t}{\sum (\rho A \bar{U})_{\text{all ports}}}$$

It was then possible to compute the mass rate of flow out of each port by the equation

$$W_p = \rho A \bar{u}$$

BIBLIOGRAPHY

LITERATURE CITED

1. Olson, F. C. W., "Flow Through a Pipe With a Porous Wall," Journal of Applied Mechanics, Vol. 16, No. 1, March, 1949, pp. 53-54.

2. Dow, Willard M., "The Uniform Distribution of a Fluid Flowing Through a Perforated Pipe," Mechanical Engineering, Vol. 72, No. 9, September 1950, p. 748.

3. Keller, J. D., "The Manifold Problem," Journal of Applied Mechanics, Vol. 16, No. 1, March, 1949, pp. 77-85.

4. Acrivos, A., B. D. Babcock, and R. L. Pigford, Flow Distributions in Manifolds, 38 pp.

5. Keller, loc. cit.

6. Acrivos, A., B. D. Babcock, and R. L. Pigford, op. cit., p. 19.

7. Stearns, R. F., R. R. Johnson, R. M. Jackson, and C. A. Larson, Flow Measurement with Orifice Meters, New York: D. Van Nostrand, Inc., 1951, pp. 102-128.

8. Schlichting, Hermann, Boundary Layer Theory, New York: McGraw-Hill Book Co. Inc. 1st ed. 1955, pp. 402-403.

9. American Society of Mechanical Engineers, Fluid Meters, Their Theory and Applications, Part 1, New York: The American Society of Mechanical Engineers, 1937, 139 pp.

OTHER REFERENCES

Jakob, Max, Heat Transfer, New York: John Wiley & Sons, Inc., 1955, Vol. 1, p. 421.

Jakob, Max and G. A. Hawkins, Elements of Heat Transfer and Insulation, New York: John Wiley & Sons, Inc., 2nd ed., 1954, pp. 13-21.

Marks, Lionel S., Mechanical Engineers' Handbook, 5th ed. New York: McGraw-Hill Book Co., Inc., 1951.

Ogle, Joseph A., Effect of Blade Design in the Louver Type Dust Separator, M.S. Thesis, Georgia Institute of Technology, School of Mechanical Engineering, 1955, 79 pp.